Improved Mode Localization in Triangular Lattices:

Light Manipulation Using Dynamic Photonic Crystals

Mostafa Shalaby* and Moustafa H. Aly
Dept. of Electronics and Communications
Arab Academy for Science, Technology, and Maritime Transport, Alexandria, Egypt
*Corresponding author: engmostafa@ieee.org

A. K. AboulSeoud
Dept. of Electrical Engineering
Alexandria University
Alexandria, Egypt

***Abstract*—Dynamic photonic crystals structures have been suggested in previous works [1-2] for optical storage and processing. By optimizing the radius of the dielectric rods in a triangular lattice structure, the present work gives maximum mode localization in the photonic bandgap. Preserving the translational invariance and adiabaticity, using the new model leads to higher bandwidth compression capabilities. While increasing the bandwidth, this design does not show significant increase in group-velocity dispersion Predictions from first principle analysis are confirmed by quantitative analysis.**

Keywords-dynamic structures; optical storage; refractive index modulation; triangular lattice; mode localization

I. INTRODUCTION

Photonic crystals (PhC) have been an area of intensive research for the past two decades. As an optical analog to semiconductors, PhC offer unprecedented capabilities for light manipulation. In an attempt to address the difficult and important problem of light storage, a dynamic PhC structure is suggested [1-2]. It is basically a coupled resonator array system which can be constructed from two-dimensional PhC structures. By modulating the refractive index of the system, it behaves as both a tunable bandwidth filter and a tunable delay element [1]. Passing the first step of simulation validation of the theory, extensive work is required in order to reach a final model for fabrication. The original model for the dynamic process is based on a two dimensional square lattice of dielectric rods with background dielectric constant of 12.25 [2]. In two dimensions, there are two other geometries that can be investigated for this application: triangular lattice and honeycomb lattice. The former has a more circular Brillouin zone than the square lattice. In this way, the bandgaps at the zone edges are easier to overlap and less index contrast is required to obtain a TM gap. While the latter can give rise to a larger gap, this requires a smaller feature length than that required for the triangular lattice at λ=1.55μm. For this reason, a triangular lattice based system is suggested in another work [3]. In the present work, this structure is optimized for optical storage and processing. By investigating the effect of the radius of the dielectric rods on the size of the photonic bandgap, an optimum radius can be used for maximum bandwidth compression capabilities of the system.

The optimum radius of the dielectric rod is found in the first part. This radius is then used to design a dynamic structure for optical storage. Structure performance is finally evaluated and compared to that of the previous structures.

II. CONSTRUCTING THE MODEL

Figure 1 shows two unit cells of the translationally invariant system used to manipulate light pulses [2]. This system consists of a waveguide side coupled to two cavities [2]. The original model consists of a square lattice of dielectric rods with a dielectric constant ε_r=12.25 and a radius r=0.2*a* embedded in air, where '*a*' is the lattice constant [4]. Preserving the two necessary conditions for using dynamic refractive index modulation, the translational invariance and adiabaticity [1], a triangular lattice structure is proposed in another work [3]. It is based on background GaAs dielectric (ε_r=11.4 at λ=1.55μm [5]) and r=0.2*a*.

An optimization of this structure for optical storage is carried out here by investigating for the optimum radius that can give a maximum gap-midgap ratio for the same dielectric material and lattice geometry.

For a triangular lattice structure with a background ε_r=11.4, Fig. 2 shows the effect of varying the rods radius on the size of the first bandgap. From the figure, the optimum radius for the background dielectric rods is r=0.17*a*. This radius corresponds to a maximum value for gap-midgap ratio $\Delta\omega/\omega_0$. $\Delta\omega$ is the bandgap size and ω_0 is the midgap frequency. This corresponds to $\Delta\omega/\omega_0$=47.7%. Compared to $\Delta\omega/\omega_0$=46.6% for the same system with r=0.2*a*, the new model offers an advantage in the defect mode localization.

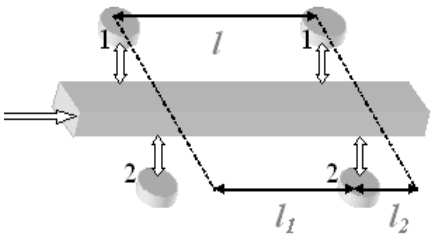

Figure 1. Schematic of two unit cells of the coupled-cavity structure used to stop light. The cavities couple to the waveguide with a coupling rate of γi.The length of the unit cell is $l = l_1 + l_2$ [2].

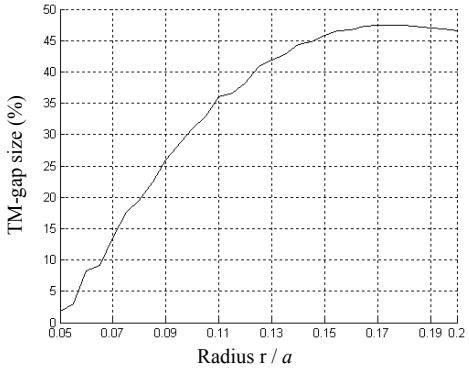

Figure 2. The effect of varying the radius of the dielectric rods on the size of the first bandgap for a triangular lattice structure (ε_r=11.4). This curve is calculated using an FDTD algorithm.

This increase in gap-midgap ratio corresponds to a bandgap size increase by 0.02μm at an operating wavelength λ=1.55 μm. Although this increase in the width of the bandgap can not be directly interpreted to an increase in the pulse compression bandwidth, this increase contributes in two ways. First, it leads to better localization of the defect modes in the bandgap. When the exponential nature of these modes is considered, a high pulse bandwidth to compress is thus obtained. Second, the quality factors for these modes increase when the gap widens.

In order to evaluate the performance of the system, both the transmission characteristics and band structure should be calculated. The intensity transmission coefficient T of the system shown in Fig. 1 can be calculated as follows [4] [6] [7]

$$T = \left(\frac{|t_1 t_2|}{1-|r_1 r_2|} \right)^2 \frac{1}{1+4\left(\sqrt{|r_1 r_2|} \Big/ \left(1-|r_1 r_2|\right) \right)^2 \sin^2\theta} \tag{1}$$

where 2θ is the round trip phase angle accumulated in the waveguide sections: θ=0.5Arg($r_1 r_2 e^{-2j\beta(\omega)l1}$), $\beta(\omega)$ is the waveguide dispersion. r_i and t_i are the reflection and transmission coefficients of the i^{th} cavity given [4] by

$$r_i = \frac{\gamma_i}{j(\omega-\omega_i)+\gamma_i} \tag{2}$$

$$t_i = \frac{j(\omega-\omega_i)}{j(\omega-\omega_i)+\gamma_i} \tag{3}$$

In order to obtain the band structure of such a system, the transmission matrix should be found a priori. If T_{ci} and T_{li} are the transmission matrices for the i^{th} waveguide side coupled to a single resonator and waveguide section respectively, (i=1, 2), the transmission matrix through an entire unit cell can be found [8] to be

$$\mathrm{T} = \mathrm{T}_{c1}\mathrm{T}_{l1}\mathrm{T}_{c2}\mathrm{T}_{l2} \tag{4}$$

where

$$\mathrm{T}_{ci} = \begin{pmatrix} 1+j/(\omega-\omega_i)\tau_i & j/(\omega-\omega_i)\tau_i \\ -j/(\omega-\omega_i)\tau_i & 1-j/(\omega-\omega_i)\tau_i \end{pmatrix} \tag{5}$$

$$\mathrm{T}_{li} = \begin{pmatrix} e^{-j\beta(\omega)l_i} & 0 \\ 0 & e^{j\beta(\omega)l_i} \end{pmatrix} \tag{6}$$

where ω_i, and $1/\tau_i$ are the resonance frequency and coupling rate to the waveguide of the i^{th} resonator. τ_i is the corresponding lifetime.

Using the above model, the band diagram for equal coupling rate cavities and ignoring any direct coupling between side cavities is found [8] to be

$$\frac{1}{2}Tr(\mathrm{T}) = \cos(kl) = \cos(\beta l) + \frac{C+}{(\omega-\omega_1)} + \frac{C-}{(\omega-\omega_2)} \tag{7}$$

where

$$C\pm = \frac{\sin(\beta l)}{\tau} \pm \frac{2\sin(\beta l_1)\sin(\beta l_2)}{(\omega_1-\omega_2)\tau^2} \tag{8}$$

This analysis is based on the representation of the eigenvalues of **T** as $e^{-jk(\omega)l}$, and $e^{jk(\omega)l}$ (because det (**T**) =1); where k is the Bloch wave vector of the entire system.

III. Model Analysis

Results obtained from simulations verify the qualitative analysis given at the beginning of the preceding section. Three systems are considered here: the original square lattice structure (ε_r=12.25 and r=0.2a) [9-10], the triangular lattice structure suggested in a previous work [3] and being optimized here (ε_r=11.4 and r=0.2a), and the optimized system proposed in this work (ε_r=11.4 and r=0.17a). The transmission characteristics are calculated using the parameters obtained from simulating these systems and using (1) – (3) given in the preceding section. While the former two systems are adjusted to have the same center frequency of ω_o=0.357 ($2\pi c/a$), this constraint is relaxed in the design of the latter for two main reasons. First, because the bandgap of the new system is frequency shifted upwards, preserving the original center frequency leads to an operating frequency range being deviated from the middle of the bandgap. In this way, the defect modes are not well localized at the center of the gap. The quality factor is reduced, and the main objective behind building this system is violated. Second, in order to study the

effect of different parameters on the system, only one is considered at a time and keeping the remaining parameters unchanged. The refractive index modulation of the cavities is kept the same for all structures. $\Delta \equiv |\omega_1 - \omega_2|\tau$ is the normalized frequency separation of the middle band for a system of cavities of resonance frequencies $\omega_{1,2} = \omega_o \pm \Delta/2\tau$ [5]. τ is the lifetime of the resonant cavities (taken to be the same for both cavities). Following the same refractive index modulation for all structures constructed in this work, simulation results can be summarized as follows. The compressible bandwidths for the square lattice, triangular lattice with r=0.2*a,* and triangular lattice with r=0.17*a* are Δ=3.189, Δ=10.129, and Δ=13.74 respectively. The transmission characteristics of both three systems are shown in Fig. 3.

The band structures calculated using (4) – (8) are shown in Fig. 4 for the three systems at the same parameters as those of the systems used to calculate the transmission characteristics. The three systems exhibit three photonic bands. The width of the middle band depends strongly on the cavities resonant frequencies. By modulating the cavities frequency spacing, the system bandwidth can be compressed as shown in Fig. 5

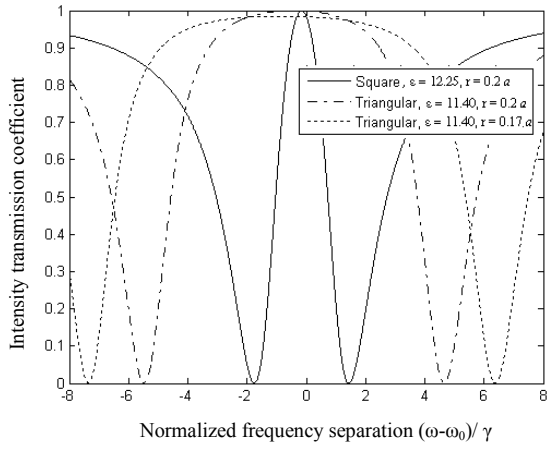

Figure 3. Transmission spectra through the coupled resonator structure for the three systems discussed.

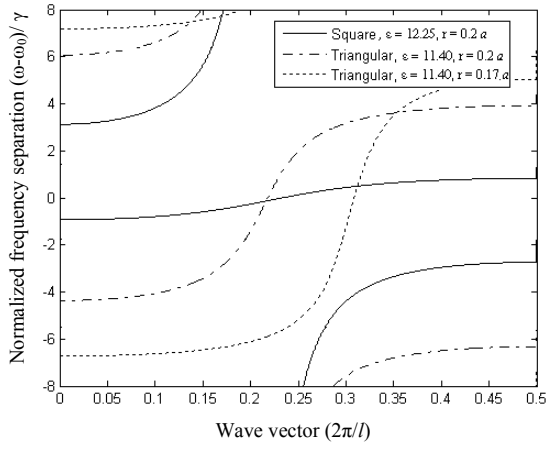

Figure 4. Band structure of the three system considered.

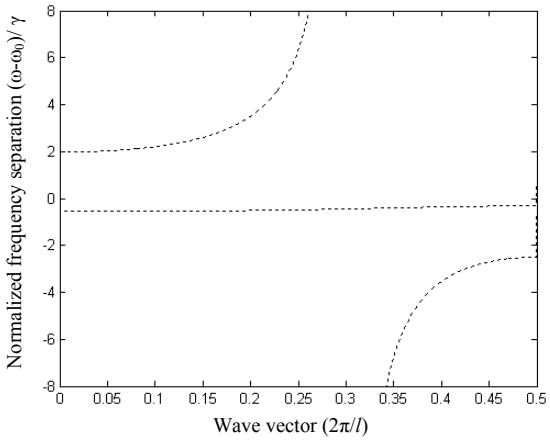

Figure 5. Band structure of the propsed model after compression.

for the new system. Figure 5 shows the possibility of compressing the bandwidth of the propagating pulse to zero and the band is thus flattened. In this way, by cascading the bandwidth filters, shown in Fig. 3, it becomes possible to reduce the group velocity of the propagating pulse to ideally zero.

Upon modulating the refractive indices of the cavities dielectric rods, these bandwidths are compressed to Δ=0.329, Δ=0.984, and Δ=1.359 respectively. This corresponds to a compression to 10.3%, 9.7%, and 9.9% of the original bandwidths in a respective order. The predictions from the quantitative analysis in the previous section are confirmed here. The compressible bandwidth increases by about 36% when the radius of the dielectric rods is reduced to 0.17 *a* for the triangular lattice system. As shown before, this is a direct result of increasing the width of the bandgap by means of optimizing the rods radius.

In order to accommodate this higher bandwidth pulse, extra length of the waveguide is required for the process. The total length of the waveguide required for the photon pulse to be stopped is determined by both a static process and a dynamic one. The static part of the length requirement can be calculated from the delay-bandwidth constraint which is independent of the signal bandwidth to be compressed. The total length *L* found in [2] can be approximated to

$$L \approx \left(\mathbf{constant} + \Delta(\tau_{\mathrm{mod}}/\tau)\right)l \qquad (9)$$

where τ_{mod} is the required time for index modulation. $(\tau_{\mathrm{mod}}/\tau)$ is taken to be constant for a given form of modulation. Therefore, a longer waveguide (interpreted as longer periods) is required to allow for sufficient index modulation. This extra length depends mainly on Δ. As an example, for the system parameters (Δ=3.2, $(\tau_{\mathrm{mod}}/\tau)$=5) previously studied [2] for a square lattice at ε=12.25, the required waveguide length in (9) is $L \approx (10+3.2*5)l$. Therefore, increasing Δ by *x%* requires increasing the length by *x**(3.2/5.2)%. The corresponding requirements are 134% (triangular lattice with r=0.2*a*) and 204% (triangular lattice with r=0.17*a*) increase in the waveguide length. It should be noted that this increase in

the waveguide length will compensate for the extra band. i.e. the final compressed bandwidth and the pulse delay are the same for both systems. Alternatively, one may not increase the waveguide length and accept the final bandwidth and pulse delay (which is worse than the results from the square lattice at ε_r=12.25). Even if a part of the waveguide length is sacrificed, there is another important factor that should be taken into consideration during system design, the group-velocity dispersion.

A waveguide carved in the bulk of PhC structure introduces a linear defect band [5]. In the design of such structures, it is important to choose a linear region of operation to avoid pulse dispersion and distortion. A slope variation ($d^2\omega/dk^2 \neq 0$) of the defect mode leads to group-velocity dispersion [5]. Figure 6 shows the band structure of the new model along with the linear defect mode. The region of operation is zoomed in and shown in Fig. 7 for this design (r=0.17*a*) and for the previous one (r=0.2*a*).

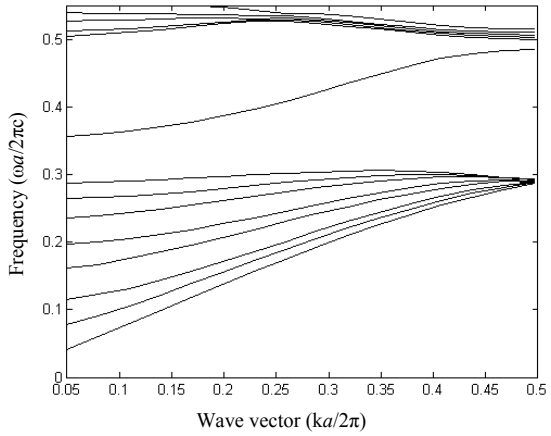

Figure 6. Band structure of a triangular lattice structure (r = 0.17 *a* and ε_r=11.4). A linear defect mode is introduced by removing a single row of rods.

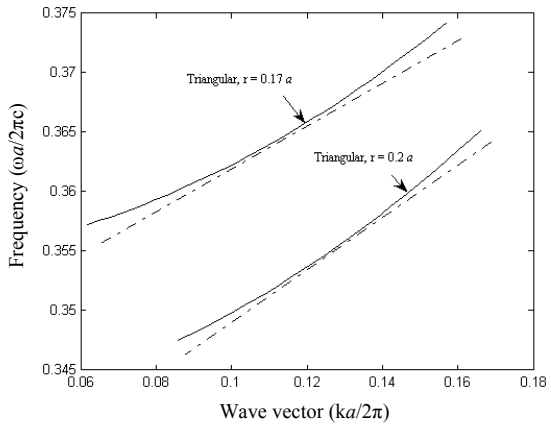

Figure 7. Group-velocity variation with respect to the perfect linear behaviour (dashed lines) in the region of interest.

Although the new design shows slightly more dispersion, this is mainly at the edges of the operating region and this effect can be taken care of when selecting the pulse shape if this region is required for operation.

IV. CONCLUSION

The highlight of this work is the optimization of dynamic PhC structures for optical storage and processing. While the original model is based on a square lattice, a triangular lattice structure shows an advantage for compressing larger bandwidth pulses [3]. An optimization of this model is carried out here by investigation for the optimum radius of the dielectric rods that leads to maximum photonic bandgap, thus improving mode localization and increasing the quality factor. This radius is found to be 0.17*a* for a triangular lattice structure made of GaAs and operating at λ=1.55μm. Using this radius to design a dynamic model shows an increase in the compressible bandwidth by 36% over the previous model with r=0.2*a*. While no significant increase in group-velocity dispersion is observed in the new model at the operating region of interest, more length of the waveguide is required to accommodate the increase in the pulse bandwidth.

REFERENCES

[1] S. Fan, M. F. Yanik, M. L. Povinelli, and S. Sandhu, "Dynamic Photonic Crystals," Optics and Photonics News, vol. 18, pp. 41-45, 2007.

[2] M. F. Yanik and S. Fan, "Dynamic Photonic Structures: Stopping, Storage, and Time-Reversal of Light," Studies in Applied Mathematics, vol. 115, pp. 233-254, 2005.

[3] M. Shalaby, A. K. AboulSeoud, and M. H. Aly, "Introducing Triangular Lattices to Dynamic Photonic Crystal Structures for Optical Storage and Processing," In press.

[4] S. Fan, "Manipulating Light with Photonic Crystals," Physica B, vol. 394, pp. 221–228, 2007.

[5] J.D. Joannopoulos, S.G. Johnson, J.N. Winn, and R.D. Meade, Photonic Crystals: Molding the Flow of Light," 2nd ed., Princeton University Press, Princeton, USA, 2008.

[6] Q. Xu, S. Sandhu, M.L. Povinelli, J. Shakya, S. Fan, and M. Lipson, "Experimental Realization of an On-chip All-Optical Analogue to Electromagnetically Induced Transparency," Phy. Rev. Lett., vol. 96, 123901, 2006.

[7] S. Fan, W. Suh, J.D. Joannopoulos, and W. Suh, "Temporal Coupled-Mode Theory for the Fano Resonance in Optical Resonators," J. Opt. Soc. Am. A, vol. 20, pp. 569-572, 2003.

[8] W. Suh, Z. Wang, and S. Fan, "Temporal Coupled-Mode theory and the Presence of Non-Orthogonal Modes in Lossless Multi-Mode Cavities," IEEE J. Quantum Electron., vol. 40, pp. 1511-18, 2004.

[9] M. F. Yanik, W. Suh, Z. Wang, and S. Fan, "Stopping Light in a Waveguide with an All-Optical Analogue of Electromagnetic Induced Transparency," Phy. Rev. Lett., vol. 93, 233903, 2004.

[10] S. Fan, M. F. Yanik, Z. Wang, S. Sandhu, and M.L. Povinelli, "Advances in the Theory of Photonic Crystals," IEEE J. Lightwave Technol., vol. 24, pp. 4493-4501, 2006.

[11] M. F. Yanik and S. Fan, "Stopping and Storing Light Coherently," Phy. Rev. A, vol. 71, 013803, 2005.